

Mössbauer studies of CuFe-72% alloy

H C Verma

Department of Physics, Indian Institute of Technology Kanpur, Kanpur 208 016
E-mail: hcoverma@iitk.ac.in

Received 15 February 2007; revised 24 July 2007; accepted 7 August 2007

Cu-Fe alloy with 72 at % of iron in powder form is prepared using simultaneous electrodeposition from a common electrolytic bath. Mössbauer spectra of the as-prepared sample show a superposition of quadrupole doublet with a large line broadening and a small component of a six line Mössbauer spectrum which has been characterized to be pure iron phase. As the samples are annealed, more and more segregation of magnetic part takes place. The linewidth and the quadrupole splitting of the residual doublet change in a correlated fashion and go through a maximum at 300°C. The crucial factor responsible for line broadening seems to be defect distribution and oxygen/hydrogen incorporation during electrodeposition and alloying. The phase-segregated iron on heating is in oxidized form (hematite and magnetite) most probably due to reaction with oxygen incorporated at the time of deposition.

Keywords: Mössbauer study, Cu-Fe-alloy, Quadrupole splitting, Mössbauer spectrum
IPC Code:G01J3/28

1 Introduction

Problems related to the formation of the metastable binary alloys having non-negative heat of formation have attracted considerable attention in recent years. Iron and copper form one of the most immiscible pair of metals at room temperature and hence numerous efforts have been undertaken to synthesize Fe-Cu alloys via non-equilibrium routes¹⁻⁶ such as covapour deposition, rapid thermal quenching, ball milling, sputtering etc. Apart from experimental investigations, Fe-Cu alloys are also studied theoretically as well as by computer simulations^{7,8}. As expected, the crystal structure for low iron concentration is found to be *fcc* and that for high iron concentrations is *bcc*. However, in intermediate range, which depends on the preparation process, the metastable alloy shows mixed *fcc* and *bcc* phase. Our group had formed Fe-Cu alloys (with iron concentration ≤ 45 at. %) using simultaneous electrodeposition from an electrolytic solution having both Fe and Cu salts⁹ and found only the *fcc* phase up to 45 at % of iron. It was observed that the structures had lots of vacancies resulting in larger QS and linewidth. Annealing of samples showed that the samples were thermally stable up to 300°C but phase segregation took place for samples with higher iron concentration at 450 and 600°C.

The preparation of Fe-Cu alloy powder by electrodeposition in high-iron range i.e, 72 at %, and study of the structural and magnetic properties of the prepared alloy using Mössbauer spectroscopy have been reported in the present paper. The as-prepared alloy has been studied using X-ray fluorescence (XRF) for elemental composition, X-ray diffraction (XRD) for crystallographic structure and phase, and Mössbauer spectroscopy for local environment around iron atoms. The phase segregation behaviour has been studied by annealing the samples at different temperatures and following the changes in Mössbauer parameters.

2 Experimental Details

Cu-Fe alloy in powder form with 72 at % of iron was prepared using simultaneous electrodeposition from a single bath using a pure platinum plate as the anode and a pure aluminium plate as the cathode. The electrolytic solution was made by dissolving $\text{Cu}(\text{NO}_3)_2 \cdot 3\text{H}_2\text{O}$ and $\text{FeSO}_4 \cdot 7\text{H}_2\text{O}$, both 99.9 % pure in distilled water. The concentration of $\text{Cu}(\text{NO}_3)_2 \cdot 3\text{H}_2\text{O}$ was 10 g/l, and that of $\text{FeSO}_4 \cdot 7\text{H}_2\text{O}$ was 70 g/l. Anode and cathode were taken in the same size, the separation between them was 2 cm and the current density was maintained at 0.01 A/cm². The potential applied during deposition was substantially more than the reduction potential of the individual constituents so that both could deposit on the cathode

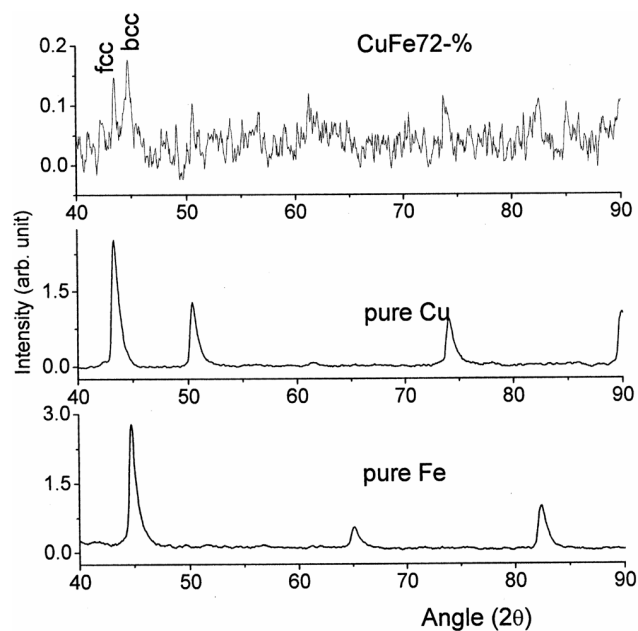


Fig. 1—X-ray diffraction patterns of as-prepared alloy along with those of pure Fe and pure Cu

simultaneously. The deposition was carried out for 10 min and then the cathode (Al plate) was taken out from the bath. It was washed several times with a gentle flow of distilled water and the material deposited was scraped gently in wet condition. This scraped material was allowed to dry in air and used as the sample for all the characterization experiments.

Relative composition of Cu and Fe in the sample was measured using AMPTEK XR-100CR X-ray fluorescence set up with an americium radioactive source. The details of system calibration, data storage and data analysis are given in our earlier work⁹. X-ray diffraction pattern was recorded on Seifert powder diffractometer using Cu-K α X-rays.

Mössbauer studies were made using conventional constant acceleration Mössbauer spectrometer coupled with 1024 channels MCS. The data analysis was done in two different ways. In one approach, discrete Lorentzian peaks were fitted to the spectra using a nonlinear least squares program developed indigenously. The uncertainty in isomer shift (IS) and quadrupole splitting (QS) are about 0.02 mm/s, in hyperfine magnetic field (HMF) about 0.2 T, and in absorption area about 2%.

3 Results and Discussion

3.1 Determination of the composition

The composition of the sample was measured using an XRF set up. The ratio of the area under the peak of

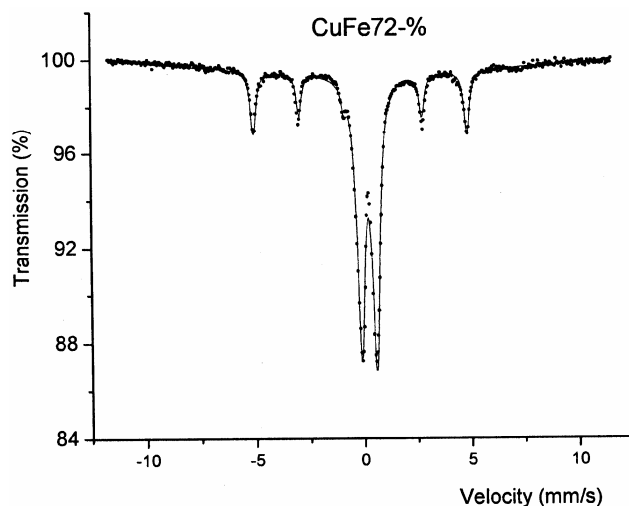


Fig. 2—Mössbauer spectrum of the as-prepared alloy recorded at room temperature

Fe ($K_{\alpha} + K_{\beta}$) and Cu ($K_{\alpha} + K_{\beta}$) in the XRF spectrum is directly proportional to the ratio of atomic concentrations of Fe and Cu in the sample. The set up was calibrated before the measurement by recording spectra for a number of Cu-Fe salt mixtures with known compositions. From the XRF studies, we find that the iron concentration in the sample is 72 at %.

3.2 X-ray diffraction

The XRD patterns for the sample prepared, for pure Fe and Cu are shown in Fig. 1. Since the *bcc* iron peak positions are distinct from the *fcc* Cu peak positions, it is easy to determine the *fcc* versus *bcc* phase in the alloy. The part crystallized shows a mixed *fcc-bcc* phase. The peaks are present at *bcc* as well as at *fcc* sites. The *bcc* peaks seem to have larger intensity than the *fcc* peaks. As the background fluctuation is large, certain humps at positions other than *fcc* Cu and *bcc* Fe cannot be ruled out. The formation of oxides or hydroxide with short range order is one possibility as the whole process of deposition and crystallization takes place in aqueous medium. Some of the material seems to be poorly crystalline giving the large background.

3.3 Mössbauer spectroscopy

Fig. 2 shows Mössbauer spectrum of the CuFe alloy recorded at room temperature. A strong doublet with a six line pattern is observed in the spectrum. While the doublet corresponds to the non-magnetic fraction comprising the fraction where iron has gone to Cu matrix either in the well crystalline *fcc* phase or in the poorly crystalline phase, the sextet corresponds

to the iron segregated in the *bcc* phase. So for the sample with 72 at % of iron, not all iron goes in copper matrix and a fraction of it segregates and forms clusters.

Table 1 presents the Mössbauer parameters of the doublet as well as for the sextet component. It is interesting to compare the Mössbauer results with the XRD pattern. The peak area for the *bcc* peak at 44.7° in the XRD pattern of CuFe72-% alloy is larger than that for the *fcc* peak at 43.2° . If we assume that X-ray peak areas are proportional to the amount of the corresponding phases present, more than half the iron in the crystalline part should form *bcc* clusters in CuFe72-% alloy. On the other hand, Mössbauer absorption area for the *bcc* Fe phase is only 25% in the spectrum of CuFe72-% alloy. Thus, X-ray diffraction seems to overweigh the *bcc* component through the structure factor or crystallinity factor and/or the Mössbauer spectrum underweighs it through the recoil-free fraction.

The quadrupole splitting in the as-prepared alloy is quite large (0.74 mm/s) as presented in Table 1. Also the linewidth is much larger than expected from a single phase. Materials deposited by electrodeposition are known to have high density of vacancies. This is because the crystal formation occurs at low temperature and hence, with low mobility of atoms. The presence of vacancies creates non-cubic environment giving a contribution to QS, and the distribution of vacancies in the system gives larger linewidths. Also the poorly crystalline part will offer different environments to iron atoms incorporated. This will increase the linewidth of the spectrum. However, the width of 0.45 mm/s, though much larger for a single phase, is not very large to suggest an amorphous kind of structure. The ordering may be of short range for XRD scales but reasonable for the binding of iron atoms to give Mössbauer effect. We suggest that the broadening is mainly due to defect incorporation which is very common in electrodeposited materials.

If we look at the sextet component in the Mössbauer spectrum of alloy, it corresponds to pure

iron metal. The linewidth of this component is 0.28 mm/s which indicates a single environment around iron nuclei. This means that the extra iron which could not go in the Cu matrix has clustered out and more importantly these clusters do not allow any vacancy, Cu atoms or foreign atoms such as oxygen, hydrogen, etc., to enter. Similar conclusions were drawn from the positron annihilation study of the sample¹⁰ CuFe72-%. One possibility for larger vacancy incorporation in Cu-Fe alloy part is that this system is thermodynamically unstable due to positive heat of formation and vacancy incorporation is needed for stabilization of the structure. On the other hand, *bcc* iron is thermodynamically very stable and good crystallization takes place even with low mobility of atoms.

3.4 Phase segregation on heating

The as-prepared alloy was annealed at 300, 450 and 600°C for 6 h under high vacuum (10^{-6} bar). Mössbauer spectra of the annealed samples are shown in Fig. 3. The magnetic phase segregation is seen to start as early as at 300°C. The area of the magnetic component increases as annealing temperature increases. It is interesting to note that even after annealing at 600°C, not all the iron has segregated as a small doublet still exists.

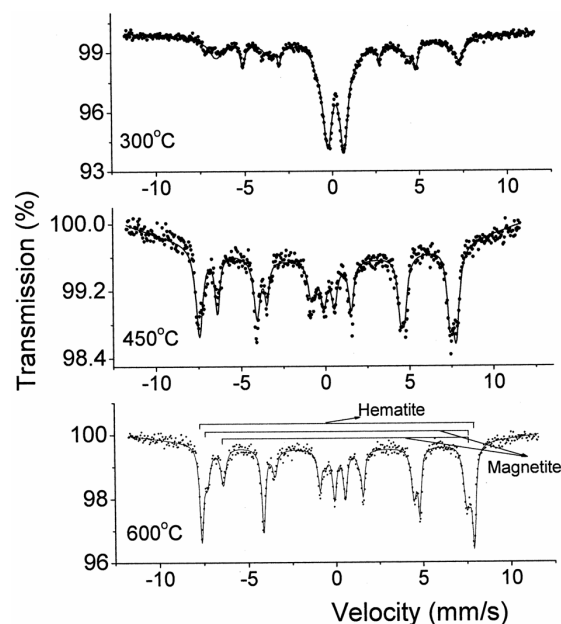


Fig. 3— Mössbauer spectra of the samples annealed at 300, 450 and 600°C for 6 hours and recorded at room temperature. The positions of the outer peaks hematite (α - Fe_2O_3) and magnetite (Fe_3O_4) are shown by marker lines in the plot of alloy annealed at 600°C

Table 1—Mössbauer parameters of the as-prepared sample, data is recorded at room temperature

Sample	IS (mm/s)	QS (mm/s)	B (T)	W (mm/s)	Area
CuFe72-%	0.34	0.74		0.45	75
	-0.002	-0.001	32.98	0.28	25

Though annealings were done in a vacuum of the order 10^{-6} bar, we get oxide phases of iron on annealing. This oxidation seems to have occurred due to phase segregation of Fe from the alloy phase and its *in-situ* reaction with oxygen that was incorporated during electrodeposition. Even annealing in running nitrogen vapour yielded oxides of iron. This means a large amount of oxygen was incorporated during electrodeposition which did not react with Fe at room temperature and was probably locked in water or oxide, hydroxide of Cu. The poorly crystalline part shown in XRD could correspond to these phases. During heating, Fe was segregated and oxygen got released from the trapped positions and reacted with iron. The phases are identified as α -Fe₂O₃ and magnetite phase (Fe₃O₄) from their Mössbauer parameters. α -Fe₂O₃ phase has an HMF of around 51.0 T and IS of around 0.33 mm/s. Well crystalline magnetite gives two sextets corresponding to the tetrahedral (A) site and octahedral (B) site in the spinel structure. The first one has HMF around 49.0 T and IS around 0.25 mm/s, and the second one has HMF around 46.0 T and isomer shift¹¹ around 0.60 mm/s. We see the inner sextet (B-site) quite clearly in the Mössbauer spectra of the alloy annealed at 450°C or 600°C, while the outer sextet (A-site) shows up as a kink in the hematite positions. It is well known that α -Fe₂O₃ is the end product of oxidation of iron if sufficient oxygen is present. All the iron is in Fe³⁺ state in this compound. The formation of Fe₃O₄ having Fe²⁺ (together with Fe³⁺) shows that supply of oxygen was not sufficient for complete oxidation of the segregated iron phase. Thus, the oxygen intake during the deposition seems to be insufficient to convert all the segregated Fe to α -Fe₂O₃. These phases are also verified by recording XRD patterns of annealed samples and the results are consistent.

3.5 Variations in linewidth and QS on heating

The variations in linewidth and QS of the doublet component with the annealing temperature (Fig. 4) show very interesting behaviour. The linewidth increases initially as the annealing temperature is increased, passes through a maximum and falls sharply to around 0.30 mm/s as the annealing temperature reaches 600°C. Similarly the QS increased first from ~0.74 to ~1.0 mm/s and finally reduced to 0.65 mm/s. It appears that the distribution of Fe/Cu atoms in the nearest neighbour shell of iron nuclei has only a small contribution in broadening. This is indicated from the fact that the linewidth for

the sample annealed at 600°C is quite low as compared to the as-prepared sample, although both have the same Cu/Fe ratio. We propose that this behaviour of QS and linewidth are due to response of vacancies as the samples get heated. At the lower annealing temperature (300°C), vacancies might have migrated and clustered. As the vacancies are clustered, they will create more deviation from cubic symmetry around the probe nuclei, increasing the QS. The increase in linewidth can also be understood as the number of different environments will increase due to vacancy clustering and their migration. When the samples are annealed at higher temperature (450 and 600°C), the QS and linewidth decrease considerably (Fig. 4). In fact, the linewidth comes to around 0.30 mm/s, close to what one expects for single-phase components. At high temperatures of annealing, the vacancies will be forced out of the system and this will decrease the QS and linewidth. Also, at higher temperatures, the randomly distributed oxygen incorporated during electrodeposition will either be expelled out (gases always have lower solubility in solids at higher temperatures) or be consumed in the oxidation of the phase-segregated iron. In either case the linewidth and QS will decrease.

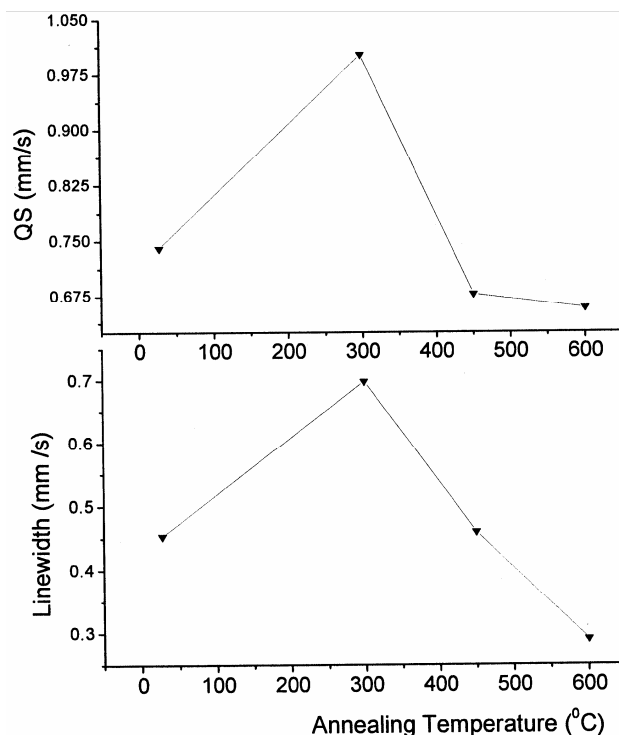


Fig. 4— Variation of linewidth and quadrupole splitting of the doublet component with annealing temperature

4 Conclusions

Iron rich CuFe-72 % alloy system in powder form has been prepared using electrodeposition. The sample prepared has a small amount of segregated iron clusters but most of the iron is dispersed in Cu matrix. Some amount of oxygen uptake has also taken place. Mössbauer spectrum of the as-prepared samples shows a quadrupole doublet with a large splitting and line broadening. The line broadening further increases as the sample is annealed, passes through a maximum and sharply falls to very small values as the annealing temperature reaches 600°C. The phase-segregated iron on heating is in oxidized form (hematite and magnetite) most probably due to reaction with oxygen incorporated at the time of deposition.

References

- 1 Mazzone G & Antisari M V, *Phys Rev B*, **54** (1996) 441.
- 2 Peng C & Dai D, *J Appl Phys*, **76** (1994) 2986.
- 3 Sumiyama K, Yoshitabe T & Nakamura Y, *J Phys Soc Jpn*, **53** (1984) 2160.
- 4 Sumiyama K & Nakamura Y, *J Magn Magn Matter*, **35** (1983) 219.
- 5 Murayama M, Takahiro K, Nagata S, Konno T & Yamaguchi S, *Surface & Coating Technology*, **83** (1986) 74.
- 6 Jiang Z, Gonser U, Gente C & Bormann R, *Appl Phys Lett*, **63** (1993) 2768.
- 7 Marian J, Wirth B D, Perlado J M, Odette G R & Rubia T Diaz de la, *Phys Rev B*, **64** (2001) 094303.
- 8 Domain C & Becquart C S, *Phys Rev B*, **65** (2001) 0241103.
- 9 Roy M K & Verma H C, *J Magn Magn Matter*, **270** (2004) 186.
- 10 Roy M K, Subrahmanyam V S & Verma H C, *Phys Lett A*, **328** (2004) 375.
- 11 Cohen R L, *Application of Mössbauer spectroscopy*, Vol I, Academic press (1976).